

# FCS DIFFUSION LAWS ON TWO-PHASES LIPID MEMBRANES : EXPERIMENTAL AND MONTE-CARLO SIMULATION DETERMINATION OF DOMAIN SIZE.

C.FAVARD, J. EHRIG, J. WENGER, P.-F. LENNE, AND H. RIGNEAULT

**ABSTRACT.** For more than ten years now, many efforts have been done to identify and characterize nature of obstructed diffusion in model and cellular lipid membranes. Amongst all the techniques developed for this purpose, FCS, by means of determination of FCS diffusion laws, has been shown to be a very efficient approach. In this paper, FCS diffusion laws are used to probe the behavior of a pure lipid and a lipid mixture at temperatures below and above phase transitions, both numerically, using a full thermodynamic model, and experimentally. In both cases FCS diffusion laws exhibit deviation from free diffusion and reveal the existence of domains. The variation of these domains mean size with temperature is in perfect correlation with the enthalpy fluctuation.

## 1. INTRODUCTION

Since the mosaic fluid concept of Singer and Nicolson [1] where lipids were considered as a "sea" in which protein were embedded, the description of biological lipid membranes has evolved to a spatio-temporal heterogeneous mixture of its own components. It is now mainly admitted that biological membranes are organized in domains of different compositions and different size including nano, meso and microscopic scale organisation. Membrane heterogeneity may be of various types. Several lipid lamellar phases have been identified in model systems. Basically, lipid bilayer can exist in solid phases ( $s$  also named gel phases  $g$ ), liquid disordered phases ( $l_d$  also named fluid phases  $f$ ), and liquid ordered phases ( $l_o$ ) which are often enriched in cholesterol. In complex lipid mixture, such as biological membranes, coexistence of these different phases may occur, leading to the formation of domains [2]. This led to the concept of *raft* as functional domains existing within biological membranes as reviewed by Simon and Ikonen [3] that highlighted their potentially ubiquitous role in cell biology. A lot of work has been done on rafts for 10 years now [4, 5, 6, 7] that led to the present consensus that rafts are heterogeneous membrane structures, rich in cholesterol and sphingomyelin and about 10 to 200 nm in diameter, highly dynamic in the lipid membranes of all eukaryotic cells [8]. Since this size is below the diffraction limit there are no direct images of their existence. Moreover, the big discrepancy founded in size mainly depends on the technique used to reveal them. For example, donor quenching FRET analysis shows nanoscale domain formation (10 to 40 nm) in lipid bilayers with a similar composition to that of the outer plasma membrane, at temperature of 37 C, whereas macroscopic phase separation was not evident [9]. Similarly,  $l_o$  nanodomains can be detected by FRET in regions of the phase diagram in which confocal microscopy indicates only the presence of a single homogenous phase [10]. Domains on length scales of 30 to 80 nm in a region of  $l_o$  and  $l_d$  co-existence have also been detected using

---

*Date:* May 3rd, 2010.

*Key words and phrases.* FCS; FCS Diffusion Laws; Monte-Carlo Numerical Simulations; Phase Separation, Domain Size Determination.

atomic-force microscopy (AFM)[11], deuterium-based nuclear magnetic resonance (2H-NMR) and differential scanning calorimetry [12, 13]. Beside their absolute size, since existence of domain in complex mixtures is dynamic, it seems relevant to use diffusion as a spatio-temporal probe of the local environment. This approach has been developed through Fluorescence Recovery After Photobleaching (FRAP) [14, 15, 16] or Fluorescence Correlation Spectroscopy (FCS) [17, 18, 19, 20] and Single Particle Tracking (SPT)[21].

Each of the dynamic microscopic techniques cited above have typical advantage and disadvantages in respect to their timescale and statistics. For example, FCS is sensitive on the millisecond to second timescale, corresponding to diffusion characteristic time in lipid mixtures of a fluorescently labeled molecule through the focus with a waist of approximately 200nm. Recently, Wawrezynieck *et al.* [22] showed that FCS was a powerful tool for analyzing complex diffusions. They showed that direct fitting of the autocorrelation function was unable to discriminate between these complex diffusions but on the opposite, exploration at different space scale allowed a more detailed view of the environment structure. They developed a variable waist FCS experiment and, based on pure numerical simulation they succeeded in reassigning different type of FCS diffusion laws as a function of the probed environment such as *rafts* or meshwork (see Fig 1). This was furthermore confirmed by measuring FCS laws in living cells [23] and use recently at different space scale down to 50 nm [24, 20]. Even though extensive numerical simulation in given geometries showed a fairly accurate prediction to what occurs in very complex systems such as cell membranes, a level of organisation in between is still missing. Therefore, investigations were conducted in order to further explore the ability of these quantitative FCS diffusion laws to distinguish phases during the transition in a well defined lipid mixture such as DMPC-DSPC.

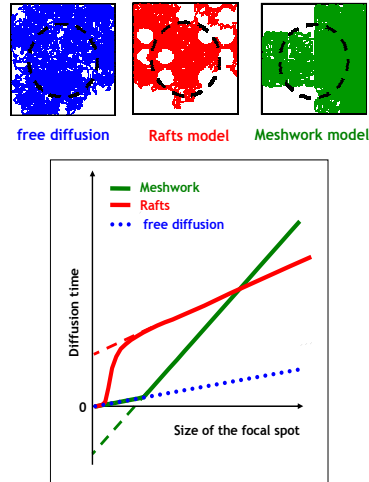


**FIGURE 1. FCS diffusion laws :** FCS diffusion laws are obtained by plotting variation of the FCS diffusion time as a function of the size of the focal spot (or waist). Here are illustrated three typical different diffusion laws obtained by numerical simulation. One for free diffusion (blue line) and two for obstructed diffusion by raft (red line) or meshwork (green line). For both obstructed diffusion models, it can be seen that FCS diffusion laws are not linear and that their asymptotic behavior can be fitted using affine model (For detailed explanations see [22]).

DMPC/DSPC lipid mixtures has been studied extensively for a while. The thermodynamic parameters of this mixture have been deciphered by many different techniques including differential scanning calorimetry, neutron scattering, NMR, ESR, Raman spectroscopy and Fourier transform infrared spectroscopy [25] or AFM [26]. The structural characteristics of this mixture has also been approached by FRAP [15, 27]. These studies have shown that DMPC-DSPC form non-ideal two-phases mixtures with small clusters of the minor phase in a continuum of the major phase. Determination of thermodynamic parameters also allowed to develop numerical simulations of the lipid mixture. Monte Carlo methods has been used to simulate the lateral distribution of each component in the pure gel or fluid phase of DMPC/DSPC mixture, firstly assuming one state and two components [28] and more recently computing a two-phases two-components triangular lattice model [29]. This model has been thoroughly used to predict size, shape and number of gel( $g$ )/fluid( $f$ ) clusters [30] and has recently been used to simulate FCS experiments on it [31].

The accuracy of the thermodynamic microscopic description of DMPC:DSPC mixtures provides the ideal model system to explore the relevancy of FCS diffusion laws. It is the scope of this paper to extend the previous works [28, 29, 30, 31] into this direction both theoretically and experimentally. Here are reported FCS diffusion laws on both DMPC:DSPC (8:2 mol:mol) mixtures and pure DMPC at different temperatures spanning the range of the phase transitions. These FCS laws shows deviations from a pure Brownian motion as expected. In order to understand the origin of this deviation and quantitatively characterize it, numerical simulations have been performed on these lipids. The results found here show that FCS diffusion laws are able to distinguish the existence of domains and that the mean size of the domains can be determined from it. A simple model is given to explain the shape of the FCS diffusion laws found here as a function of diffusion in a solid or a liquid environment.

## 2. MATERIAL AND METHODS

**2.1. Material.** The lipids 1,2-distearoyl-*sn*-glycero-3-phosphocoline (DSPC) and 1,2-dipalmitoyl-*sn*-glycero-3-phospho-choline (DMPC) were purchased from Avanti Polar Lipids (Alabaster, AL.). They were used without further purification and kept at  $-20^{\circ}\text{C}$  in chloroform:methanol(9:1, mol:mol) at 100mM concentration. For FCS measurements lipids mixtures were labeled with 2-(4,4-difluoro-5,7-dimethyl-4-bora-3a,4a-diaza-s-indacene-3-pentanoyl)- 1-hexadecanoyl-*sn*-glycero-3-phosphocholine( $\beta$ -BODIPY FL C5-HPC)from Invitrogen (Carlsbad, CA, USA)).

**2.2. Monte Carlo simulation of the two phases two components lipid mixture.** Our Monte Carlo simulations were directly adapted from the work of Sugar *et al.* [29] also described in [31]. Briefly, the thermal fluctuations of the DMPC : DSPC lipid mixture was simulated using a two-state Ising type monolayer triangular lattice. Each lattice point is occupied by one acyl chain of either DMPC or DSPC. During the simulation, trial configuration are generated by means of six different elementary steps :

- One that can be described as a **phase transition step**, consists in changing the state of a randomly selected acyl chain from gel to fluid or inversely.
- Five that can be described as **diffusion steps**, consist in exchanging two neighboring molecules. In the Monte Carlo algorithm, 3 different processes can occur at 3 different time scales. One is diffusing in a liquid environment, the other is diffusing in gel environment and the last is changing its state. For lipids within a mixed environment (both gel and fluid) the probability of entering a diffusion step depends on the fraction of gel lipids chains ( $f_{c,g}$ ) surrounding the two lipids that

are to enter a diffusion step. As extensively described in [31], a rate function  $r(f_{c,g})$  has been introduced in the simulation :

$$(1) \quad r = r_0 \exp(-f_{c,g} \frac{\Delta E}{kT})$$

where  $r_0$  is the value of  $r$  in a fully liquid environment ( $f_{c,g} = 0$ ) and  $\Delta E$  is the energy barrier needed for a diffusion step in an all-gel environment ( $f_{c,g} = 1$ ). As in the work of Hac *et al.* [31], the phase transition step probability ( $r_{state}$ ) was set to be equal to  $r_0$  and  $\Delta E/kT$  was set to 4.25 according to the following ratio :  $\frac{D_f}{D_g} = 70$

The Monte-Carlo simulations were implemented in C++ (Microsoft Visual C++ Version 6.0). They were run on a multiprocessor computer (4 AMD opterons dual-core 865 at 1.8 Ghz) using the Intel C++ compiler (icc v10.0). For each type of simulations periodic boundary conditions were used. For the lipid mixture, simulations were made on 8:2 mol:mol DMPC-DSPC lipid mixtures at different temperatures (294, 298, 299, 300, 301, 302, 304, 306, 308, 310, 315 and 325 K). A 60x60 lipids lattice (60x120 lipid chains) (1 lipid=1 lattice unit square) was simulated. For DMPC alone, a 40x40 lipid lattice (40x80 lipid chains) was used.  $10^8$  Monte Carlo steps were made for each simulation except at 294 K ( $1.2 \cdot 10^8$ ).

**2.2.1. Thermodynamic model.** The thermodynamic model used here is extensively described in [29] and [31] Briefly, each lipid chains can exist in two states, gel( $g$ ) of fluid( $f$ ), these states being different in internal energy as well as in entropy. Therefore the total energy of one layer of the lipids in a given configuration  $C$  is given by :

$$(2) \quad \begin{aligned} E(C) = & n_A^g E_A^g + n_A^f E_A^f + n_B^g E_B^g + n_B^f E_B^f \\ & + n_{AA}^{gg} E_{AA}^{gg} + n_{AA}^{gf} E_{AA}^{gf} + n_{AA}^{ff} E_{AA}^{ff} + n_{AB}^{gg} E_{AB}^{gg} \\ & + n_{AB}^{gf} E_{AB}^{gf} + n_{AB}^{fg} E_{AB}^{fg} + n_{AB}^{ff} E_{AB}^{ff} + n_{BB}^{gg} E_{BB}^{gg} + n_{BB}^{gf} E_{BB}^{gf} + n_{BB}^{ff} E_{BB}^{ff} \end{aligned}$$

where  $n_{A,B}^g$  and  $n_{A,B}^f$  are the numbers of the gel and fluid lipid chains and the  $E_{A,B}^g$  and  $E_{A,B}^f$  terms are the respective internal energies of the two states of species A and B. It is shown in [29] that the Gibbs free energy for a given state can be written as :

$$(3) \quad \begin{aligned} G = & G_0 + n_A^f (\Delta H_A - T \Delta S_A) + n_B^f (\Delta H_B - T \Delta S_B) \\ & + n_{AA}^{gf} \omega_{AA}^{gf} + n_{BB}^{gf} \omega_{BB}^{gf} + n_{AB}^{gg} \omega_{AB}^{gg} + n_{AB}^{ff} \omega_{AB}^{ff} + n_{AB}^{gf} \omega_{AB}^{gf} + n_{AB}^{fg} \omega_{AB}^{fg} \end{aligned}$$

Where  $\Delta H_A$  and  $\Delta H_B$  the calorimetric enthalpies,  $\Delta S_A = \frac{\Delta H_A}{T_{m,A}}$  and  $\Delta S_B = \frac{\Delta H_B}{T_{m,B}}$  are the respective melting entropies with  $T_{m,A}$  and  $T_{m,B}$  being the melting temperatures of the two pure components and  $G_0$  the energy of an all gel lipid matrix. All the other parameters ( $\omega_{ij}^{\alpha\beta}$ ) are the nearest-neighbor interaction parameters of a lipid chain species  $i$  in state  $\alpha$  with a lipid chain species  $j$  in state  $\beta$ . The whole set of parameter described above has been given values according to [31] since these values has been obtained on multilamellar vesicles. These values are summarized in table 1.

**2.2.2. FCS diffusion laws in the simulation.** In order to build FCS diffusion laws in the MC simulations, 20% of the total number of DMPC lipids chains were introduced as markers. During the simulation, these lipids move and generate intensity according to their position in the laser profile which is considered as a Gaussian with a given waist  $w$  (value of the radius at  $1/e^2$  intensity),

$T_{m,A} = 297.1K$	$\omega_{AA}^{gf} = 1353J.mol^{-1}$
$T_{m,B} = 327.9K$	$\omega_{BB}^{gf} = 1474J.mol^{-1}$
$\Delta H_A = 13.165kJ.mol^{-1}$	$\omega_{AB}^{gg} = 607J.mol^{-1}$
$\Delta H_B = 25.37kJ.mol^{-1}$	$\omega_{AB}^{ff} = 251J.mol^{-1}$
$\Delta S_A = 44.31J.mol^{-1}.K^{-1}$	$\omega_{AB}^{gf} = 1548J.mol^{-1}$
$\Delta S_B = 77.36J.mol^{-1}.K^{-1}$	$\omega_{AB}^{fg} = 1716J.mol^{-1}$

TABLE 1. Monte-Carlo simulation parameters. Parameters of the Monte Carlo simulation of DMPC-DSPC mixture. The indices  $g$  and  $f$  correspond to gel and fluid state respectively. Values are the one given in [31]

$$(4) \quad I(r) \propto \exp\left(-\frac{2(r-r_0)^2}{w^2}\right)$$

At each time step, the detected intensity in our simulations is computed assuming a Poisson distribution. The number of detected photons ( $n_{ph}$ ) for a particle at position (x,y) is given by a random variable following the Poisson distribution with parameter  $\beta I(x,y)$  with  $\beta$  describing the collection efficiency of the setup [32].

To analyse intensity fluctuations, the normalized time autocorrelation function (ACF) is defined as :

$$(5) \quad g^{(2)}(\tau) = \frac{\langle n_{ph}(t)n_{ph}(t+\tau) \rangle}{\langle n_{ph}(t) \rangle^2}$$

where  $\langle . \rangle$  represent a time average. In our simulations, the ACF is calculated from a generated intensity file after the whole Monte Carlo simulation. The software correlator used to compute the ACFs follows the architecture proposed by [33] and described in [32]. It has a logarithmic timescale, each channel having an individual sampling time and delay time.

FCS diffusion laws are then built by correlating the intensity fluctuations obtained at different waist in the same simulation. The biggest waist being 2/3 of the simulated matrix.

**2.3. Image analysis.** While running Monte-Carlo simulations, some images of the lattice were recorded at a chosen Monte Carlo step frequency, using an intensity code for the four different combination of the lipids states ( $I_{gf}^{AB}$ ). This lead in easier numerical image analysis capacities for thresholding.

Image correlation spectroscopy analyzes were conducted on thresholded binary images using the ICS plugin for ImageJ ([http : //rsb.info.nih.gov/ij/](http://rsb.info.nih.gov/ij/)) developed by Fitz Elliott, based on the work of Petersen [34] which can be found at [http : //www.cellmigration.org/resource/imaging/software](http://www.cellmigration.org/resource/imaging/software). Using spatial image correlation spectroscopy module of the plugin generated a 2D correlogram of our images obtained from the MC simulation. This 2D correlogram was reduced to a monodimensional correlogram assuming a circular symmetry. The 1D correlogram was arbitrary fitted by the following exponential function :

$$(6) \quad g(\xi) = g(0)(a_1.e^{-(\xi/l_{c1})} + a_2.e^{-(\xi/l_{c2})}) + g(\infty)$$

where  $l_{c2}$  is the characteristic length of the domains. Correlograms were average over 50 different images at different time steps of the MC simulation at each temperature. The performance of this procedure was tested using simulated images of circular domains of different radius and showed error within 20 % accuracy.

Direct morphoanalysis was also performed using the ImageJ plugin "particle analysis". Analysis are conducted on binary thresholded image over a set of 50

different images obtained at different time of the MC simulation as for ICS. The "particle analysis" plugin is a simple binary derivative method that delimits areas of pixels having the same value (1 or 0) therefore giving a direct access to the number and area of the domains on each image. This method allows to plot the exact distribution in term of area and occurrence of the domains. For simplicity reason, it was decided to only keep the mean area of the domains defined as the following :

$$(7) \quad A_{dom} = \frac{1}{N} \sum_{A=2}^{A=\infty} N_A A$$

with A the value of the area (discretised in classes every 25 pixels) and N the number of occurrence of this area within the image.

Finally, the fractional area of gel lipids ( $S_g^n$ ) defined as the following  $S_g^n = \frac{S_g}{S_g + S_f}$  within the image could also be determined at each temperature using this method, allowing therefore to scale the image in nm. This fraction was used to extrapolate the total area of the simulation and the mean area ( $\langle a \rangle = f_g \cdot a_g + f_l \cdot a_l$ ) occupied by a lipid according the following value of lipid areas,  $a_f = 63 \text{ \AA}^2$  and  $a_g = 45 \text{ \AA}^2$  for PC lipids [14, 35].

**2.4. Preparation of multilamellar vesicles.** 10  $\mu\text{l}$  of a 10mM mixture of DMPC:DSPC (8:2 mol:mol) labeled with  $\beta$  Bodipy Fl C5-HPC at a lipid molar ratio of 1:50 000 were deposited on a glass coverslip previously extensively cleaned with ethanol, water:ethanol (7:3 vol:vol) and chloroform. Lipids were dried under vacuum for one hour and hydrated with 700  $\mu\text{l}$  of pure distilled water previously heated at 50 °C. Sample was then allowed to cool down for at least 30 min to the different measurement temperatures within the microscope chamber.

**2.5. FCS experiments.** FCS experiments were performed on a home-built device. This experimental setup has been extensively described in [24] . Briefly, it is based on an inverted microscope (Zeiss Axiovert 35M) with a NA=1.2 water immersion objective (Zeiss C-Apochromat) and a three-axis piezo-scanner (Physik Instrument, Germany). In order to avoid photobleaching of the fluorescent label during the experiment 3  $\mu\text{W}$  of a CW laser at 488nm was used for fluorescence excitation. For experiments above the diffraction limit, a 30  $\mu\text{m}$  pinhole conjugated to the microscope object plane, defined the observation volume. After the pinhole, the fluorescence signal is split by a 50/50 beamsplitter and focused on two avalanche photodiodes (Perkin-Elmer SPCM-AQR-13) through a  $535 \pm 20 \text{ nm}$  fluorescence bandpass filters (Omega Filters 535DF40). The fluorescence intensity fluctuations are analyzed by cross-correlating the signal of each photodiode with a ALV6000 hardware correlator. For FCS diffusion laws, waist of the laser in the object plane was modified by underfilling the microscope objective back-aperture using an adjustable diaphragm placed on the excitation optical path. The values of the observation area therefore obtained were calibrated by measuring the diffusion time of a 0.5  $\mu\text{M}$  Rhodamine-6G in aqueous solution at 22 °C ( $D=280 \mu\text{m}^2 \cdot \text{s}^{-1}$ ). For each waist at each temperature of the study, at least 200 FCS measurements of 5s duration each were made by series of 10.

**2.6. Fitting of ACFs.** For free Brownian two-dimensional diffusion in the case of a Gaussian molecular detection efficiency and accounting for negligible photophysics effects on the fluorophore (triplet state, blinking, bleaching...) the fluorescence autocorrelation function (ACF) is given by :

$$(8) \quad g^{(2)}(\tau) = 1 + \frac{1}{N} \frac{1}{1 + \frac{\tau}{\tau_d}}$$

where  $N$  denotes the average number of molecules in the observation area and  $\tau_d$  the diffusion time.  $\tau_d$  is linked to the laser beam transversal waist  $w$  and the molecular diffusion coefficient  $D$  by :

$$(9) \quad \tau_d = \frac{w^2}{4D}$$

All the ACFs obtained experimentally using variable waist above diffraction limit, or on Monte-Carlo simulation were fitted using Eq. 8.

### 3. RESULTS

**3.1. FCS at variable radii and variable temperature on DMPC and DMPC:DSPC samples.** FCS diffusion laws were acquired on pure DMPC lipid multilamellar vesicles and on vesicles made of DMPC:DSPC (8:2 mol:mol) both labeled with C5-Bodipy-PC at different temperatures below, within and above the phase transitions. Fig 2 A shows a typical correlogram obtained on pure DMPC at 297K with a transversal waist  $w=218 \mu\text{m}$ , Fig 2 B shows the same type of experimental correlogram obtained on the DMPC:DSPC 8:2 mol:mol mixture at 302K with a transversal waist  $w=210 \mu\text{m}$ . On both part of the figure, the red line is the fit of the correlogram using Eq. 8 allowing determination of  $\tau_d$  in the correlogram. The residual, which is plotted in the upper part of Fig 2 A and B, confirms the quality of the fit. Repeating experiments at different waists and different temperatures allows to obtain FCS diffusion laws. These are depicted in Fig 2 C and D for pure DMPC and DMPC:DSPC mixture respectively.

FCS diffusion laws can be fit at different temperatures using the following equation :

$$(10) \quad \tau_d = \frac{w^2}{4D_{eff}} + \tau_{d_0}$$

with  $\tau_d$  the experimental values of diffusion time at different waist  $w$  and  $\tau_{d_0}$  the extrapolated diffusion time at  $w^2 = 0$ . These FCS diffusion laws also allow the determination of an effective diffusion coefficient named  $D_{eff}$ . Fig. 10 A and B at the end of this paper show the increase of this diffusion coefficient  $D_{eff}$  with temperature for both sample.

As illustrated in Fig 3 A and B, fit of the experimental FCS diffusion laws exhibit a negative  $\tau_{d_0}$  for temperatures below the phase transition (Fig 3 A,  $T < 297K$ ) in the case of DMPC or below the second transition ( $gf : ff$ ) in the case of the DMPC:DSPC mixture (Fig 3 B,  $T < 310K$ ). When the FCS laws are acquired in pure fluid phase ( $T > 310K$  for DMPC:DSPC mixture or  $T > 298K$  for DMPC alone), they exhibit  $\tau_{d_0}$  values close to zero which shows a pure Brownian behavior of the diffusing molecules as expected. When plotting these  $\tau_{d_0}$  value as a function of temperature, it can be seen on Fig 3 C and D that in both cases (DMPC alone or lipid mixture) the more the system is in the gel phase (or the more the temperature decrease) the more  $\tau_{d_0}$  becomes negative.

In order to confirm the experimental results and to understand the origin of a negative  $\tau_{d_0}$  when gel domains are present in a fluid phase, it was decided to perform Monte Carlo simulations using a full set of thermodynamic parameters for DMPC and DMPC:DSPC lipid mixtures.

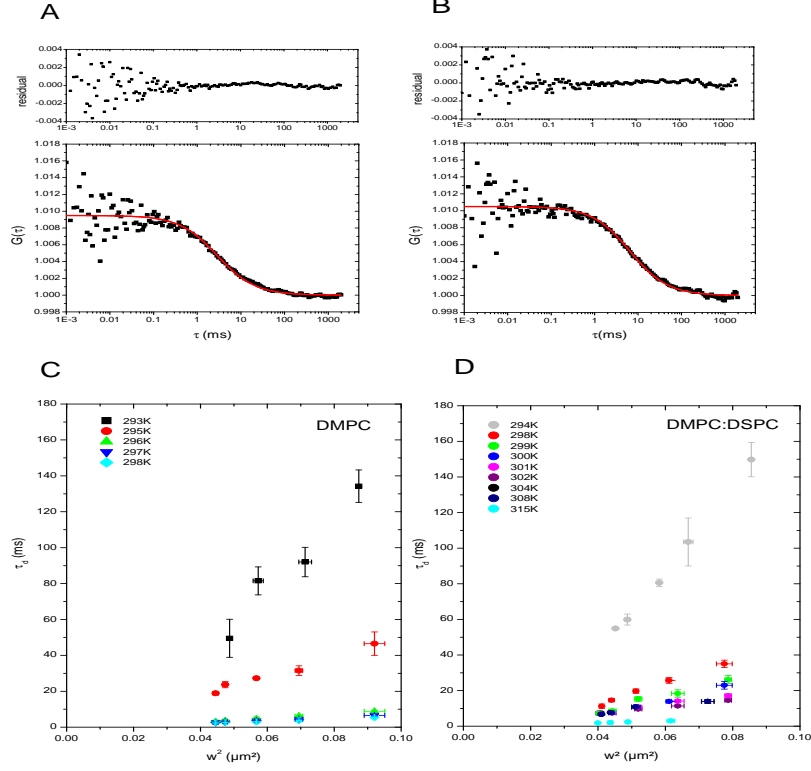
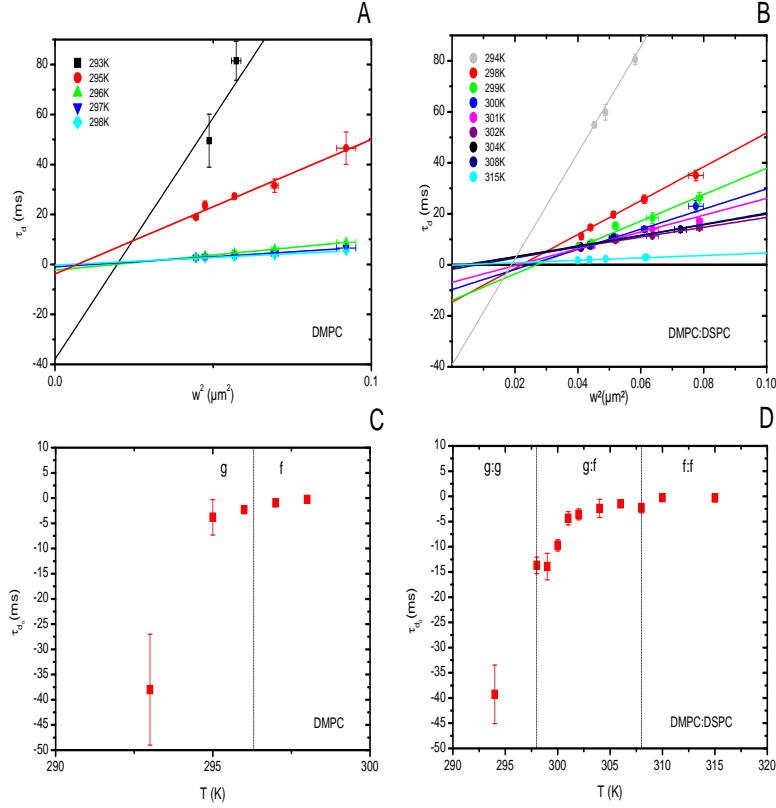


FIGURE 2. **Experimental correlograms and FCS diffusion laws obtained on lipid mixtures.** **Part A and B** Correlograms obtained on multilamellar vesicles of DMPC (Part A) and DMPC:DSPC 8:2 mol:mol (Part B) (square dots are experimental data) fitted using eq. 8. Residuals are plotted in the upper part of the figure showing accuracy of the fit. **Part C and D** Experimental FCS diffusion laws obtained for DMPC (Part C) and DMPC:DSPC 8:2 mol:mol (Part D) at different temperatures. (Colors on line)

### 3.2. FCS at variable radii on MC numerical simulations : Diffusion Laws.

Monte Carlo simulation were made at different temperature below, within and above the two state transitions ( $gg : gf : ff$ ) of the DMPC:DSPC 8:2 (mol:mol) and below, within and above phase transition of DMPC alone ( $g : f$ ). Fig 4A shows a snapshot of the DMPC:DSPC 8:2 mol:mol mixture at 304K ( $gf$  state) as obtained from the MC simulation. Gel domains (in green) can be seen in a sea of fluid lipids (in red)(60x120 lipid chains). MC simulated correlograms of this mixture are depicted for different waist at this temperature in Fig 4B, showing an increase of  $\tau_d$  with increasing waists as expected. As seen from experiments (see Fig 3),  $\tau_d$  is also expected to increase with decreasing temperature at a given waist, this is illustrated in Fig 4C, confirming the validity of our MC simulations. At low temperature ( $T < 300K$ ) or large waist ( $w > 20l.u.$ ) the correlation function at long time scale shows higher noise due to the limited number of events arising at these times. Nevertheless, the determination of  $\tau_d$  is still valid. FCS diffusion laws could therefore be established here again by plotting  $\tau_d$  as a function of the square of the waist  $w^2$ .

As illustrated in Fig. 5 FCS diffusion laws are obtained for the different temperature of the MC simulations for both DMPC:DSPC mixture (Fig. 5A) and DMPC



**FIGURE 3. Variation of experimental  $\tau_{d0}$  as a function of temperature.** **Part A and B** Fit of the experimental FCS diffusion laws using eq. 10 for DMPC (Part A) and DMPC:DSPC 8:2 mol:mol (Part B) allowing determination of  $\tau_{d0}$  for each set of data. **Part C and D**  $\tau_{d0}$  is plotted against temperature for DMPC (part C) and DMPC:DSPC 8:2 mol:mol (part D). Square dots are obtained value with error bar. (Colors on line)

alone (Fig. 5B). As found experimentally in the case of DMPC:DSPC mixture, above 310 K the FCS laws seems perfectly linear (Fig 5 A), accounting for a pure Brownian diffusion of the lipids. Below 310 K (Fig 5 A inset) all the FCS laws seems to be biphasic, exhibiting therefore deviations from a pure Brownian diffusion as expected for inhomogeneous media. Even below the first transition temperature gg : gl of the lipid mixture these FCS laws still shows a biphasic behavior. As shown in fig. 5 B the same biphasic type of FCS diffusion laws has been obtained with pure DMPC MC simulations below the transition temperature (296.5 K).

MC simulated FCS diffusion laws can be fit using the equation 10 as depicted in Fig. 6 A for DMPC:DSPC mixture and in Fig. 6 B for DMPC alone.

As in the experiments, the value of an effective diffusion coefficient  $D_{eff}$  can be calculated following Eq. 10 and is plotted as a function of temperature in supplementary material Fig 10 C (DMPC:DSPC mixture) and D (DMPC alone). In both case, it is important to note that the global shape of the curve  $D_{eff} = f(T)$  is the same for simulation and experiments and is signed by a sharp increase during the transition from gel to fluid medium.

It can be seen that, as in the experimental FCS diffusion laws,  $\tau_{d0}$  decrease with decreasing temperature as plotted in Fig. 6C and D respectively for DMPC:DSPC

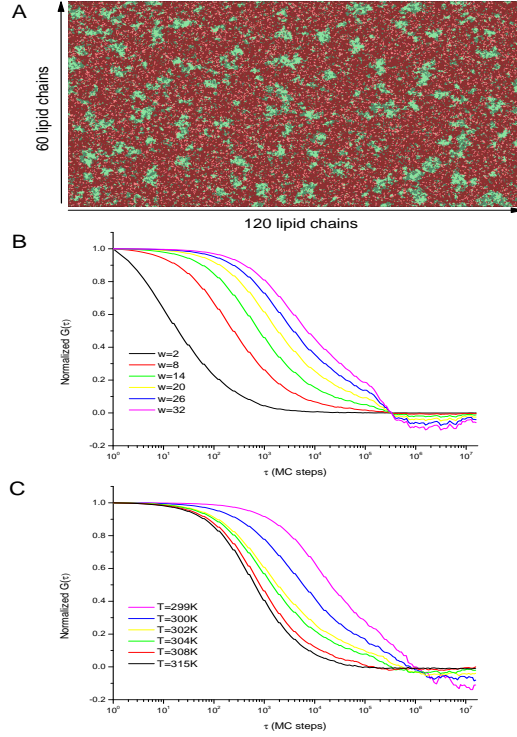
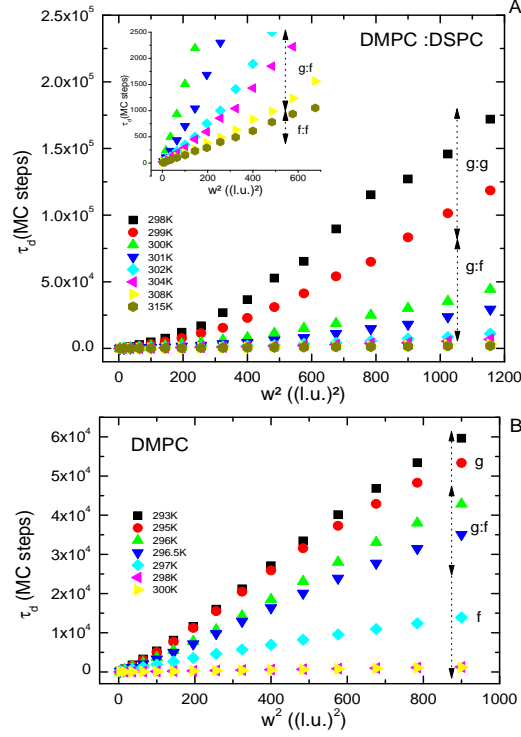


FIGURE 4. **Images and Correlograms obtained by MC simulation of DMPC-DSPC 8:2 mol:mol mixture.** **Part A.** Monte-Carlo snapshot of a 60x60 lipids lattice 8:2 mol:mol DMPC-DSPC mixture at 304K. Green domains correspond to gel lipids, red domains to fluid lipids. **Part B.** Normalized correlograms obtained from the Monte-Carlo simulation at 304K for different waists. **Part C.** Normalized correlogram obtained from the Monte-Carlo simulation at a given waist ( $w=8$  l.u.) at different temperatures from gel ( $T < 300K$ ) to liquid ( $T > 315K$ ) and within the melting regime ( $300K < T < 315K$ ).

mixture and DMPC alone. These  $\tau_{d_0}$  also reach values close to zero at  $T \geq 310K$  for the DMPC:DSPC mixture or  $T \geq 298K$  for DMPC alone, confirming a pure Brownian diffusion of the system above this temperature.

These observations confirm the validity of our experimental results on both DMPC and DMPC:DSPC lipid mixture. Both system exhibit deviation from a pure Brownian motion as soon as they are not in pure fluid state. These deviations can be seen using FCS diffusion laws and are signed by a negative  $\tau_{d_0}$ .

**3.3. Origin of negative diffusion time at zero waist.** As shown above in Fig 3C and D or Fig 6C and D,  $\tau_0$  extrapolated from the fit of the FCS diffusion laws (both experimental and simulated) using eq 10 exhibit growing negative value with decreasing temperature. This result is surprising since it is different from the one obtained by Wawrezynieck *et al* [22] in the case of microdomains (where  $\tau_{d_0}$  is positive) since DMPC/DSPC mixture domains would have been expected to behave similarly. The results obtained here are closer to the one obtained in this previous study for meshworks (see Fig 1 for comparison). In this later case, Wawrezynieck *et al* [22] shown that the FCS diffusion law could be correctly described by the following equations :



**FIGURE 5. FCS diffusion laws obtained from MC simulation at different temperatures.** **Part A** FCS diffusion laws obtained from MC simulated DMPC-DSPC 8:2 mol:mol mixture are represented for different temperature below, within and above the melting regime of the mixture. Onset shows an enlargement for low waists at high temperature. These FCS diffusion laws exhibit two slopes at low temperature but starts to be linear with a null origin at temperature above 310K, indicating a pure Brownian diffusion process. **Part B** FCS diffusion laws obtained from MC simulations of pure DMPC are represented for different temperature below and above phase transition (296.3K). FCS diffusion laws exhibit here again two slopes below the phase transition and starts to be linear with a null origin at temperature above 298K.

$$(11) \quad \tau_d = \begin{cases} \frac{w^2}{4D_{micro}} & \text{if } X_c^2 < 2 \\ S_{conf} \frac{w^2}{4D_{micro}} + k(\tau_d^{domain} - \tau_{conf}) & \text{if } X_c^2 > 2 \end{cases}$$

Where  $D_{micro}$  is the local diffusion coefficient,  $\tau_d^{domain}$  is the characteristic diffusion time inside a mesh,  $\tau_{conf}$  is the confinement time defined as  $S_{conf}\tau_d^{domain}$  and  $S_{conf}$  is the strength confinement that is a function of the probability to cross a barrier to go from one mesh to another, giving therefore an indication on the stiffness of the barrier.  $X_c^2$  being the normalized coordinates of the waist( $w$ ) to the meshsize ( $r$ ) and defined in the case of a square meshwork as  $X_c^2 = \frac{\pi w^2}{4r^2}$ . It has to be noted that for  $X_c^2 > 2$  eq 11 can be rewritten as :

$$(12) \quad \tau_d = S_{conf} \frac{w^2}{4D_{micro}} + k\tau_d^{domain}(1 - S_{conf})$$

In the case of the DMPC/DSPC mixture, one can simplify the system to a two state (gel and fluid) system with for each a typical diffusion time  $\tau_d^g$  and  $\tau_d^f$  exist. It has to be noted that at least for the MC simulation, at a given waist,  $\tau_d^g = 70\tau_d^f$ . Since  $\tau_d^g$  is much bigger than  $\tau_d^f$ , when a tracer moves into a gel environment it

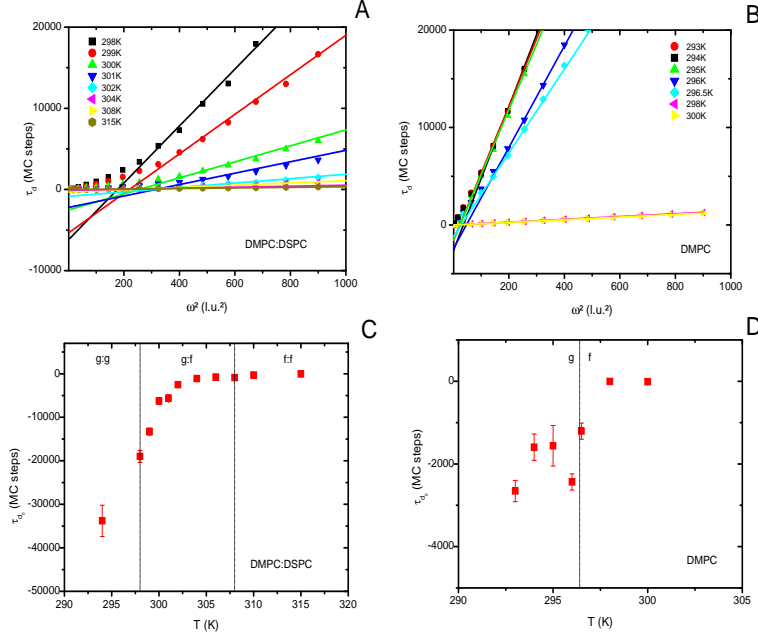


FIGURE 6. Variation of  $\tau_{d0}$  obtained by simulations as a function of temperature. **Part A and B.** Fit of the asymptotic part of the FCS diffusion law using eq 10 at different temperatures for DMPC:DSPC 8:2 mol:mol (part A) and DMPC (part B). **Part C and D.**  $\tau_{d0}$  is plotted against temperature for DMPC:DSPC 8:2 mol:mol (part C) and DMPC (part D). Square dots are obtained value with error bar. A sharp increase is seen around 300K, close to the first meting temperature of the DMPC-DSPC 8:2 mol:mol mixture (part C) and around 296K, close to the melting temperature for DMPC.

can appear as being strongly confined to this environment as compared to the same tracer into a fluid environment. Therefore, gel domains can be considered as barriers to free diffusion of the molecule in the liquid phase. It can be clearly seen from a movie generated using images step by step in the simulation (data not shown) that the tracer molecules move freely in the fluid environment while they seem to be unable to cross a gel environment at least during the duration of the movie (300 MC steps). Therefore, by analogy to the meshwork case described here above,  $\tau_{conf}$  could be defined as a function of  $\tau_d^g$  times the normalized surface of gel ( $S_g^n$ ) that has to be crossed by the tracer molecule.

FCS diffusion law obtained here could be described by the following simple intuitive model :

$$(13) \quad \tau_d = \begin{cases} \frac{w^2}{4D_{micro}(T)} & \text{if } w^2 < aw_0^2 \\ S_g^n \frac{w^2}{4D_{micro}(T)} + K(\tau_d^f - S_g^n \tau_d^g) & \text{if } w^2 > aw_0^2 \end{cases}$$

With  $K$  and  $a$  given constants and  $w_0^2$  the value of  $w^2$  for  $\tau_d = 0$ .

Eq 13 shows that the first part of the the FCS diffusion law, below the cross over regime, is linked to the local diffusion constant  $D_{micro}$  which is a function of the temperature. In the MC simulation,  $D_{micro}$  has been defined such that  $D_{micro}^f = 70D_{micro}^g$ . By linear fit of the simulated FCS laws at small waists ( $w^2 < 300l.u.^2$ ),  $D_{micro}$  can be found for each temperature and it can be found that in the case of MC simulation  $D_{micro}(325K) = 70D_{micro}(294K)$  (data not shown). If one extrapolate the value of  $D$  from the second part of the FCS diffusion law ( $300l.u.^2 < w^2 <$

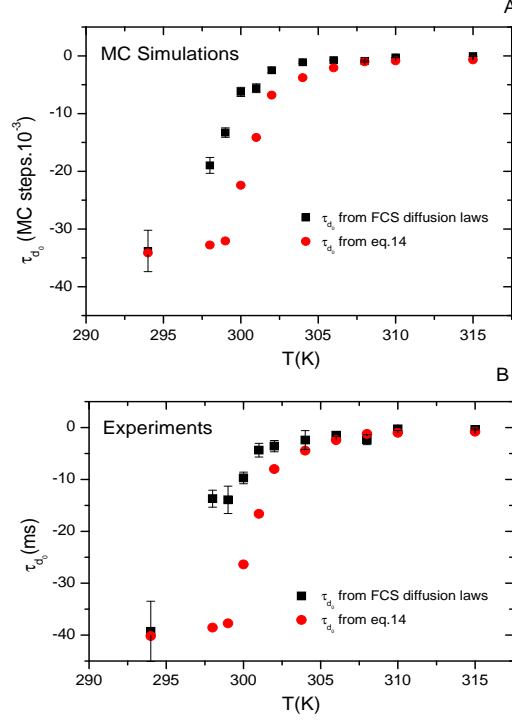


**FIGURE 7. Comparison of experimental and MC simulated  $\tau_{d0}$  to  $\tau_{d0}$  from eq. 14. Part A.** Comparison of  $\tau_{d0}$  obtained by linear fit of the asymptotic part of the simulated FCS diffusion laws to  $\tau_{d0}$  obtained by eq. 14 as a function of temperature ( i.e. a function of normalized gel area). **Part B.** Comparison of  $\tau_{d0}$  obtained by linear fit of the asymptotic part of the experimental FCS diffusion laws to  $\tau_{d0}$  obtained by eq. 14 as a function of temperature. Both are normalized by means of K factor at 294K.

$1200l.u.^2$ ), then it is found that  $D_{micro}(325K) = 160D_{micro}(294K)$ . This confirms that the shape of the second part of the FCS diffusion law does contain more than only free diffusion. This cannot be verified for experimental laws since the first part of the FCS law is not accessible.

As defined above,  $\tau_{d0}$  is the value of  $\tau_d$  for  $w^2 = 0$ . From eq 13 it is found that :

$$(14) \quad \tau_{d0} = K\tau_d^f(1 - 70S_g^n)$$

With increasing temperatures, the relative normalized solid area ( $0 < S_g^n < 1$ ) is decreasing down to zero. In this study,  $S_g^n$  was determined from MC simulation of the DMPC/DSPC mixture at different temperatures. Figure 7 shows the evolution of  $\tau_{d0}$  with temperature for MC simulated FCS diffusion laws (Fig. 7 A) and experimental FCS diffusion law (Fig. 7 B) and the calculated values of  $\tau_{d0}$  as a function of  $S_g^n$  according to eq. 14, adjusted to the lowest temperature value of  $\tau_{d0}$  by K constant. Both figures 7 A and B show a nice adequation of the calculated values with eq. 14 and the numerical or experimental obtained values, confirming the hypothesis that solid domains act as barriers to free-diffusion of the tracers. Although the present model is rather heuristic than accurate, it suggests that the gel confinement areas can be viewed as meshwork barriers for the diffusion of fluorescent reporters, but not as impermeable domains, or as raft-like domains.

**3.4. Determination of domain size.** Wawrezynieck *et al* [22] have previously shown that deviation from a pure linear regime in the FCS diffusion laws were a signature of heterogeneities in the probed environment. They also showed that the crossover regime in the FCS diffusion laws was a function of the relative size of both the probing waist and the domain size. In the case of mesh restriction to diffusion, Eq. 11 shows that the FCS diffusion law could be described by two linear laws crossing over each other close to the mesh size, therefore authorizing measurement of it. The FCS diffusion laws obtained from MC simulations in this study can also be described by two linear laws crossing over at a given waist, exhibiting a cross over regime which is a putative function of the domain size.

These MC simulated FCS laws were analysed by a simple linear fit of the highest slope of the curves (from  $300l.u.^2 < w^2 < 1200l.u.^2$ ), using equation 10, since the first part of the curve is not accessible experimentally and therefore the cross over regime cannot be directly determined. Nevertheless, eq 13 shows that the cross-over regime should occur at  $aw_0^2$ . Since  $w_0^2$  is the parameter that can be easily determined from both simulations and experiments, it seemed important to estimate in which extent it is related to the size of domains.

For this purpose, snapshots of the simulations as the one depicted in Fig 4 A were made at different temperatures for the DMPC:DSPC lipid mixture. These images were analyzed by ICS and by direct space morphoanalysis as described previously.

In the case of ICS analysis, all images between the two main phase transitions were analyzed using a biexponential function with two characteristics ( $l_{c1}$  and  $l_{c2}$ ) coherence lengths. It appeared that, in that case,  $l_{c1}$  varied between 0.5 and 1 ( $l.u.$ )<sup>2</sup> which is a value equivalent to one chain or one lipid and indeed the smallest motif the image can contain. Whereas for the direct space morphology analysis, domain representing less than two lipids were not taken into consideration. Comparison of values found for each methods are made by measuring the number of lipids in the domains. This is directly obtained on the morphoanalysis and estimated by FCS and ICS in supposed circular domains of area  $\pi l_{c2}^2$  or  $\pi \frac{\sqrt{w_0^2}}{2}$ . There are no fundamental reasons for choosing circular domains except simplification for the comparison of each analysis. Indeed the snapshot of the simulations clearly shows that the domains are not circular nor square but have a very complex geometry, which has been already shown in detail by Sugar *et al.* [36].

Using surface area of  $a_f = 63\text{\AA}^2$  and  $a_g = 45\text{\AA}^2$  for PC lipids respectively in fluid phase or gel phase [14, 35] allowed calculation of the mean radius of domains in nm. In Fig 8 are plotted the mean radius in nm of the above defined domains obtained by FCS diffusion laws on the MC simulation and compared to those viewed by ICS analysis or direct space morphoanalysis. This comparison shows that the mean domains radius obtained by our FCS diffusion laws are close to the one found both by morphoanalysis and by ICS analysis. This clearly shows that the  $w_0^2$  is an indirect indication of the mean radius of the domains.

Moreover, Fig 9A, that shows changes in the experimental  $w_0^2$  and the mean radius ( $w_0/2$ ) parameters found by FCS diffusion laws as a function of temperature, exhibits a main change between 301 and 302 K (close to the first melting temperature, transition  $gg : gf$ ) and a smaller shoulder around 306 K (close to the second melting temperature, transition  $gf : ff$ ). The shape of the  $w_0^2 = f(T)$  curve is similar to the heat capacity profile of the DMPC:DSPC (8:2 mol:mol). This is also seen in FCS diffusion laws of DMPC alone (Fig 9B). In that case,  $w_0^2$  (equivalently  $w_0/2$ ) show an increased at 296K, close to the  $g : f$  phase transition temperature of DMPC(*ref*). This variation of  $w_0^2$  is also obtained in simulated FCS diffusion laws of DMPC:DSPC mixture and DMPC alone respectively (Fig 9C and Fig 9D). Whereas radius ( $w_0/2$ ) of domains viewed by FCS diffusion laws on MC simulations

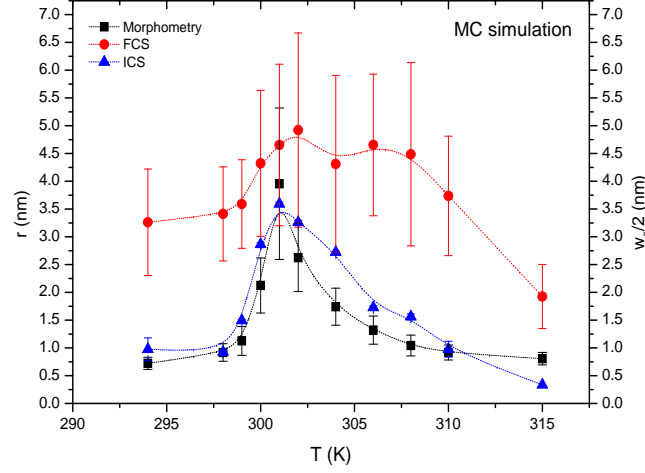


FIGURE 8. **Comparison of  $w_0^2$  obtained by three different methods as a function of temperature.** Three different methods (see text for details) were used to determine the mean size of the domains within the MC simulation of DMPC:DSPC 8:2 mol:mol mixture. These methods are compared as a function of temperature. Circles are the values obtained by determination of  $w_0^2$  in FCS diffusion laws. It has to be noted that variation of the domain size seen by ICS of FCS diffusion laws shows strikingly similarities with heat capacity profile (for comparison see Fig 8.6 p135 of [37])

were found to be less than 5 nm, experimental FCS diffusion laws shows values of  $w_0^2$  values between 10 000 and 26 000 nm<sup>2</sup> for the lipid mixture, which finally give values of  $w_0/2$  higher than 50 nm and lower than 80 nm.

#### 4. DISCUSSION

Diffusion in this type of lipid mixture has been studied for a long time by various techniques. Vaz *et al.* performed FRAP experiments [15] on DMPC: DSPC 8:2 mol:mol at different temperatures using NBD-DLPE as the fluorescent dye and found values ranging from  $D=0.25 \mu\text{m}^2.\text{s}^{-1}$  at  $T=293\text{K}$  to  $D=7.5 \mu\text{m}^2.\text{s}^{-1}$  at  $T=308\text{K}$ . The experimental FCS diffusion laws obtained in this study exhibit value of diffusion coefficient between  $0.12 \mu\text{m}^2.\text{s}^{-1}$  at  $294\text{K}$  to  $5.6 \mu\text{m}^2.\text{s}^{-1}$  at  $310\text{K}$ . Indeed, the global increase of  $D$  obtained by FCS diffusion laws as a function of temperature is coherent with the one observed using FRAP technique. In complex media, FRAP measurements generally do not show total fluorescence recovery. This is described by fitting FRAP recovery curves with a so-called immobile fraction. This immobile fraction reflects the incapacity for one molecule to leave the photodestructured area during the time of the experiment and is therefore an indirect information on the restriction to the diffusion. Immobile fraction is ranging between 0 (free diffusion) and 1 (no diffusion). In their study, Vaz *et al.* showed that the immobile fraction varied from 0.52 at  $293\text{K}$  to 0 at  $308\text{K}$  with a sharp transition in between, closely linked to the phases transitions  $gg : gl : ll$  of the lipid mixture [15]. The FCS diffusion laws observed in our study exhibit non zero and negative  $\tau_{d_0}$  below the second transition  $gl : ll$ . It has to be pointed out that the shape of the evolution of the immobile fraction as a function of the temperature of the lipid mixture is strikingly similar to the evolution of our  $\tau_{d_0}$  parameter. In a pure gel phase, one would expect to retrieve a free diffusion behavior of the molecules.

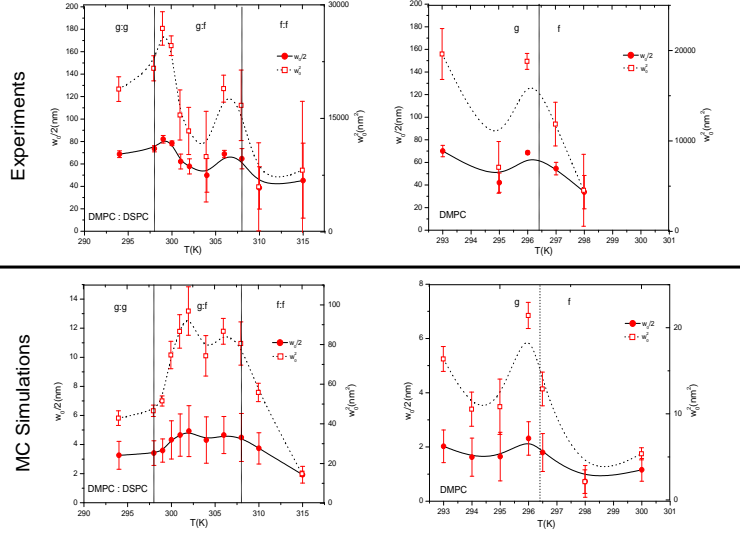


FIGURE 9. Variation of  $w_0^2$  and  $w_0/2$  as a function of temperature for MC simulated DMPC-DSPC mixture or pure DMPC.  $w_0^2$  is estimated from the linear fit using eq. 10 of the FCS diffusion law as the value of  $w^2$  for  $\tau_d = 0$ . Here is depicted plots of  $w_0^2$  (right scale) and  $w_0/2$  (left scale) as a function of temperature determined experimentally on a DMPC:DSPC 8:2 mol:mol mixture (Part A) or pure DMPC (Part B) or numerically for DMPC:DSPC 8:2 mol:mol (Part C) and pure DMPC (Part D). (Experimental point are linked by a solid curve (for  $w_0/2$ ) or dashed curve (for  $w_0^2$ ) polynomial fit to guide the eye.)

In this later case, the immobile fraction, as well as our  $\tau_{d0}$  parameter should go back to the zero value. This is not the case here, neither it is the case for the immobile fraction in the study of Vaz *et al.* [15]. One simple explanation could be that the system is not in pure gel state at a temperature close to 294K. But the MC simulation using the thermodynamics of the system shows that more than 99% of the system is in the gel state. When this amount of gel is present in the mixture, percolation is expected to occur and to stop long range diffusion, which is the main diffusion component seen in our FCS experiments. Nevertheless, it has been suggested that even in gel state, ripple phase formation allows fast diffusion along line defects [38]. This would lead to fast fluctuations within the observed area and therefore a higher diffusion coefficient than expected. For example, Hac *et al.* [31] also found using FCS a value of diffusion coefficient in the gel phase in the range of  $0.05$  to  $0.1 \mu\text{m}^2.\text{s}^{-1}$  which is again significantly higher than the one reported by other methods. Ripple phase formation is certainly not the only explanation of these high diffusion coefficients found in the gel phase since our MC simulations exhibit exactly the same behavior regarding the  $\tau_d^0$  parameter as experiments do, regardless the fact that ripple phases do not exist in the simulations. Lipid state change could also be a source of fluorescence fluctuations within a given area and therefore lead to a new correlation time. The system studied here exhibits three different time scales : one characteristic of diffusion in a pure liquid environment ( $\tau_d^l$ ), one in a pure gel environment ( $\tau_d^g$ ) and finally one proportional to the rate of state change from liquid to solid (or inversely) for each lipid chains. It has been shown that this latter time has an influence on the apparent diffusion [31, 30]. If state changes occur more rapidly than the time needed for a tracer to diffuse into a gel obstacle, the obstacle itself will be able to fluctuate and to change his shape

and size. This is equivalent to diffusion in smooth obstacle where it has been shown that percolation has a much smaller effect than expected [39]. Finally, time scale of the method is also very important. FCS or FRAP experiments are conducted over tenths of seconds which does not authorize, at diffraction limited spots, to measure  $D$  lower than  $10^{-4}$  or  $10^{-5} \mu m^2.s^{-1}$ . All these possibilities can explain the finding of a higher diffusion coefficient than the one intuitively expected and a non zero  $\tau_d^0$  in the pure gel phase at 294K.

Another parameter of interest in our FCS diffusion laws is the value of the intercept of asymptotic linear extrapolation of the diffusion law with the abscissa axis. This parameter is empirically defined has the "zero diffusion time" characteristic waist (value of  $w^2$  at  $\tau_d = 0$ ,  $w_0^2 = \frac{-\tau_{d0}}{4D_{eff}}$ ). This empirical parameter has been analysed has a function of temperature. It exhibits a very good correlation to the differential scanning calorimetry curve with two maxima located at the same temperature (1K accuracy) for DMPC:DSPC 8:2 mol:mol and one maximum at 296K for DMPC alone. Liquid or solid domains are known to be maximum in size at the maximal enthalpy [40, 41], it seemed therefore reasonable to analyse this  $w_0^2$  parameter as being a function of the domain size. Wawrezinieck *et al* [22] have shown by using classical random walk simulations, that in given geometries, this parameter allows to estimate the exact size of the mesh or the domain. These numerical simulations results have been confirmed by analytical solving of the problem by N. Destainville [42]. The geometry of the system studied here is totally unknown and depends only on the thermodynamic properties of it. Therefore it seems very difficult to obtain an analytical model that precisely define the size of the domains as a function of  $w_0^2$ . Nevertheless, by using ICS or morphometry analysis of the images obtained from the MC simulation, it is shown here that the radius of circular-like domains found in the images is close to the size of those estimated by means of the  $w_0^2$  parameter obtained from the FCS diffusion laws. This clearly shows that  $w_0^2$  is a good estimator of the size of the domains in the lipid mixture. In this study, circular-like domains are found to measure between 2.5 to 5 nm in radius in the case of MC simulations while they exhibit size in between 50 to 80 nm in experiments. AFM studies on a 50:50 mol:mol DMPC:DSPC supported bilayers lipid mixture has shown to exhibit domain size between 50 (circular) and 150x300 nm (rectangular) in the  $g : f$  phase coexistence [43]. These values are coherent with the one observed here experimentally for our 80:20 mol:mol DMPC:DSPC lipid mixtures. Gliss *et al.* [44] also showed existence of nanoscale domains in DMPC-DSPC mixture. AFM imaging allowed them to measure gel domains of 10 nm, while neutron diffraction permitted identification of gel domains exhibiting values of 7 nm. These size are comparable to the one observed here in our MC simulations whether by ICS analysis or by estimation of the  $w_0^2$  parameter in the simulated FCS diffusion laws.

As stated above, this two-phases two-components DMPC:DSPC lipid mixture has been studied for a long time by many different techniques both on dynamic and structural approaches. Bagatolli *et al.* [45] even showed existence of micrometer size domains within GUVs made of DMPC:DSPC 1:1 mol:mol.

Indeed, all these observations show that such systems exhibit different space and time scale confinement, rising the question of the anomaly of the diffusion. Anomalous diffusion has been extensively used to describe and study many different type of dynamic behavior of biological molecules in their complex media (for review see [46]). Basically, it can be seen as a general case for diffusion. Relation between time and space could be generalized as  $\langle r^2 \rangle \propto t^\alpha$ , with  $0 < \alpha < 2$ . If  $\alpha = 1$ , the diffusion is normal and described by pure Brownian motion whereas if  $\alpha < 1$  the system is sub-diffusive indicating that the molecular motions are

restricted. DMPC:DSPC two-phases two-components lipid mixture has been described by means of anomalous diffusion both on MC simulation [30] and experimentally [31]. In this case,  $\alpha$  was found to be systematically less than one, except in the  $f : f$  region and in the far  $g : g$  region (very low temperature), where the molecular motion becomes Brownian again. FCS diffusion laws obtained on both MC simulations and experiments have also been fitted using anomalous diffusion. In this study,  $\alpha$  has been found to vary between 0.64 and 1 in both cases (MC simulations and experiments) exhibiting two minima at the phase transitions  $g : g \rightarrow g : f$  and  $g : f \rightarrow f : f$  (data not shown). Anomalous diffusion can therefore clearly describe the molecular motion in this two-phases two-components lipid mixtures or during phase transition in a pure lipid, nevertheless, even if it gives informations on the heterogeneity of the systems, it fails to quantitatively interpreted the structure of this heterogeneous medium. It has been a deliberate choice all along this work to compare results at extremely low spatial scale (MC simulation) with experimental scale, this later being 3 orders of magnitude larger. This is motivated by anomalous properties of diffusion in the lipid mixture that exhibit similar space and time behavior at any scale. This question of time to space invariance can also be viewed *a posteriori* by the consistency of the results found here ( $w_0$  versus T for example) although simulations and experiments are compared at very different scales.

## 5. CONCLUSION

Here is presented a study of the two-phases two-components DMPC:DSPC 8:2 mol:mol lipid mixture and pure DMPC lipid system by means of FCS diffusion laws both experimentally and using MC simulation with a complete thermodynamic description. It is clearly shown that these FCS diffusion laws, allows quantitative characterization of the system in terms of diffusion, phase transition and mean size of the gel or fluid domains presents in the lipid mixture. Domain size and transient confinement times has already been shown to be predictable by the use of FCS diffusion laws on defined geometries and pure random walk model [22]. Here it is shown that this can be generalized to a more complex model where the geometry is unknown and the molecular motion are only driven by the thermodynamic parameters of the system itself. Finally, the parameter obtained from the interpretation of the FCS diffusion laws issued of the numerical simulation are shown to have the same behavior than the one obtained on experimental system. This confirms the advantages of using FCS diffusion laws on experimental systems to described their temporal and spatial structure.

## REFERENCES

- [1] SJ Singer and GL Nicolson. Fluid mosaic model of structure of cell-membranes. *Science*, 175(4023):720–&, 1972.
- [2] D. A. Brown and E. London. Structure and origin of ordered lipid domains in biological membranes. *J. Membr. Biol.*, 164:103–114, 1998.
- [3] K Simons and E Ikonen. Functional rafts in cell membranes. *Nature*, 387(6633):569–572, 1997.
- [4] D. A. Brown and E. London. Structure and function of sphingolipid- and cholesterol-rich membrane rafts. *J. Biol. Chem.*, 275:17221–17224, 2000.
- [5] S. Mukherjee and F. R. Maxfield. Membrane domains. *Annu. Rev. Cell Dev. Biol.*, 20:839–866, 2004.
- [6] K. Simons and W. L. Vaz. Model systems, lipid rafts, and cell membranes. *Annu. Rev. Biophys. Biomol. Struct.*, 33:269–295, 2004.
- [7] K. Jacobson, O. G. Mouritsen, and R. G. Anderson. Structure and function of sphingolipid- and cholesterol-rich membrane rafts. *Nat. Cell Biol.*, 9:7–14, 2007.
- [8] Linda J. Pike. Rafts defined: a report on the Keystone Symposium on Lipid Rafts and Cell Function. *J. Lip. Res.*, 47(7):1597–1598, 2006.

- [9] J. R. Silvius. Fluorescence energy transfer reveals microdomain formation at physiological temperatures -in lipid mixtures modeling the outer leaflet of the plasma membrane. *Biophys. J.*, 85:10341045, 2003.
- [10] G. W. Feigenson and J. T. Buboltz. Ternary phasediagram of dipalmitoyl-PCdilauroyl-PCcholesterol:nanoscope domain formation driven by cholesterol. *Biophys. J.*, 80:27752788, 2001.
- [11] C. Yuan, J. Furlong, P. Burgos, and L. J. Johnston. The size of lipid rafts: an atomic force microscopy study of ganglioside GM1 domains in sphingomyelinDOPCcholesterol membranes. *Biophys. J.*, 82:25262535, 2002.
- [12] Y. W. Hsueh, K. Gilbert, C. Trandum, M. Zuckermann, and J. Thewalt. The effect of ergosterol on dipalmitoylphosphatidylcholine bilayers: a deuterium NMR and calorimetric study. *Biophys. J.*, 88:1799–1808, 2005.
- [13] S. L. Veatch, I. V. Polozov, K. Gawrisch, and S. L. Keller. Liquid domains in vesicles investigated by NMR and fluorescence microscopy. *Biophys. J.*, 86:29102922, 2004.
- [14] PFF Almeida, WLC Vaz, and TE Thompson. Lateral diffusion and percolation in 2-phase, 2-component lipid bilayers - Topology of the solid-phase domains inplane and across the lipid bilayer. *Biochemistry*, 31(31):7198–7210, 1992.
- [15] WLC Vaz, ECC Melo, and TE Thompson. Translational diffusion and fluid domain connectivity in a 2-component 2-phase phospholipid bilayer. *Biophys. J.*, 56(5):869–876, 1989.
- [16] WLC Vaz and PF Almeida. Microscopic versus Macroscopic diffusion in one-component fluid phase lipid bilayer-membranes. *Biophys. J.*, 60(6):1553–1554, 1991.
- [17] J Korchach, WW Webb, and GW Feigenson. Two-color fluorescence correlation spectroscopy to detect motional heterogeneity over nanoscopic distances in giant unilamellar vesicles. *Biophys. J.*, 82(1, Part 2):2473, 2002.
- [18] Salvatore Chiantia, Jonas Ries, and Petra Schwille. Fluorescence correlation spectroscopy in membrane structure elucidation. *BBA-Biomembranes*, 1788:225–233, 2009.
- [19] J Korchach, P Schwille, WW Webb, and GW Feigenson. Characterization of lipid bilayer phases by confocal microscopy and fluorescence correlation spectroscopy (vol 96, pg 8461, 1999). *Proc. Nat. Am. Sc.*, 96(17):9966, 1999.
- [20] C. Eggeling, C. Ringemann, R. Medda, G. Schwarzmann, K. Sandhoff, S. Polyakova, V. N. Belov, B. Hein, C. von Middendorff, A. Schoenle, and S. W. Hell. Direct observation of the nanoscale dynamics of membrane lipids in a living cell. *Nature*, 457(7233):1159–U121, 2009.
- [21] C Dietrich, B Yang, T Fujiwara, A Kusumi, and K Jacobson. Relationship of lipid rafts to transient confinement zones detected by single particle tracking. *Biophys. J.*, 82(1):274–284, 2002.
- [22] L Wawrezinieck, H Rigneault, D Marguet, and PF Lenne. Fluorescence correlation spectroscopy diffusion laws to probe the submicron cell membrane organization. *Biophys. J.*, 89(6):4029–4042, 2005.
- [23] Pierre-Francois Lenne, Laure Wawrezinieck, Fabien Conchonaud, Olivier Wurtz, Annie Boned, Xiao-Jun Guo, Herve Rigneault, Hai-Tao He, and Didier Marguet. Dynamic molecular confinement in the plasma membrane by microdomains and the cytoskeleton meshwork. *EMBO J.*, 25(14):3245–3256, 2006.
- [24] J Wenger, F Conchonaud, J Dintinger, L Wawrezinieck, T.W. Ebbesen, H. Rigneault, D. Marguet, and P-F. Lenne. Diffusion analysis within single nanometric apertures reveals the ultrafine cell membrane organization. *Biophys. J.*, 92(3):913–919, 2007.
- [25] M. Fidorra, T. Heimburg, and H. M. Seeger. Melting of individual lipid components in binary lipid mixtures studied by FTIR spectroscopy, DSC and Monte Carlo simulations. *Biochem. Biophys. Acta*, 1788(3):600–607, 2009.
- [26] MC Giocondi and C Le Grimellec. Temperature dependence of the surface topography in dimyristoylphosphatidylcholine/distearoylphosphatidylcholine multibilayers. *Biophys. J.*, 86(4):2218–2230, 2004.
- [27] V Schram, HN Lin, and TE Thompson. Topology of gel-phase domains and lipid mixing properties in phase-separated two-component phosphatidylcholine bilayers. *Biophys. J.*, 71(4):1811–1822, 1996.
- [28] N Jan, T Lookman, and DA Pink. On computer-simulation methods used to study models of 2-component lipid bilayers. *Biochemistry*, 23(14):3227–3231, 1984.
- [29] IP Sugar, TE Thompson, and RL Biltonen. Monte Carlo simulation of two-component bilayers: DMPC/DSPC mixtures. *Biophys. J.*, 76(4):2099–2110, 1999.
- [30] IP Sugar and RL Biltonen. Lateral diffusion of molecules in two-component lipid bilayer: A Monte Carlo simulation study. *J. Phys. Chem. B*, 109(15):7373–7386, 2005.
- [31] AE Hac, HM Seeger, M Fidorra, and T Heimburg. Diffusion in two-component lipid membranes - A fluorescence correlation spectroscopy and Monte Carlo simulation study. *Biophys. J.*, 88(1):317–333, 2005.

- [32] T Wohland, R Rigler, and H Vogel. The standard deviation in fluorescence correlation spectroscopy. *Biophys. J.*, 80(6):2987–2999, 2001.
- [33] K. Schatzel. New concepts in correlator design. In *Institute of Physics Conference Series*, pages 175–184. Hilger, London, 1985.
- [34] NO Petersen, PL Hoddellius, PW Wiseman, O Seger, and KE Magnusson. Quantitation of membrane-receptor distribution by image correlation spectroscopy - Concept and application. *Biophys. J.*, 65(3):1135–1146, 1993.
- [35] MC Wiener, RM Suter, and JF Nagle. Structure of the fully hydrated gel phase of dipalmitoylphosphatidylcholine. *Biophys. J.*, 55(2):315–325, 1989.
- [36] IP Sugar, E Michanova-Alexova, and PLG Chong. Geometrical properties of gel and fluid clusters in DMPC/DSPC bilayers: Monte Carlo simulation approach using a two-state model. *Biophys. J.*, 81(5):2425–2441, 2001.
- [37] T. Heimburg. Thermal biophysics of membranes. In *Tutorials in Biophysics*, page 135. Wiley-VCH, Berlin, 2007.
- [38] MB Schneider, WK Chan, and WW Webb. Fast diffusion along defects and corrugations in phospholipid  $P_\beta$  liquid crystals. *Biophys. J.*, 43:157–165, 1983.
- [39] S. Torquato. Random Heterogeneous Media: Microstructure and Improved Bounds on Effective Properties. *Appl. Mech. Rev.*, 44:37–76, 1991.
- [40] T. Heimburg. Mechanical aspects of membrane thermodynamics. Estimation of the mechanical properties of lipid membranes close to the chain melting transition from calorimetry. *Biochem. Biophys. Acta*, 1415:147–162, 1998.
- [41] H. Ebel, P. Grabitz, and T. Heimburg. Enthalpy and volume changes in lipid membranes. I. The proportionality of heat and volume changes in the lipid melting transition and its implication for the elastic constants. *J. Phys. Chem. B.*, 105:7353–7360, 2001.
- [42] N. Destainville. Theory of fluorescence correlation spectroscopy at variable observation area for two-dimensional diffusion on a meshgrid. *Soft Matter*, 4:1288–1301, 2008.
- [43] MC Giocondi, L Pacheco, PE Milhiet, and C Le Grimallec. Temperature dependence of the topology of supported dimirystoyl-distearoyl phosphatidylcholine bilayers. *Ultramicroscopy*, 86:151–157, 2001.
- [44] C Gliss, H Clausen-Schaumann, R Gunther, S Odenbach, O Randl, and TM Bayerl. Direct detection of domains in phospholipid bilayers by grazing incidence diffraction of neutrons and atomic force microscopy. *Biophys. J.*, 74(5):2443–2450, 1998.
- [45] LA Bagatolli and E Gratton. A correlation between lipid domain shape and binary phospholipid mixture composition in free standing bilayers: A two-photon fluorescence microscopy study. *Biophys. J.*, 79:434–447, 2000.
- [46] James A. Dix and A. S. Verkman. Crowding effects on diffusion in solutions and cells. *Ann. Rev. Biophys.*, 37:247–263, 2008.

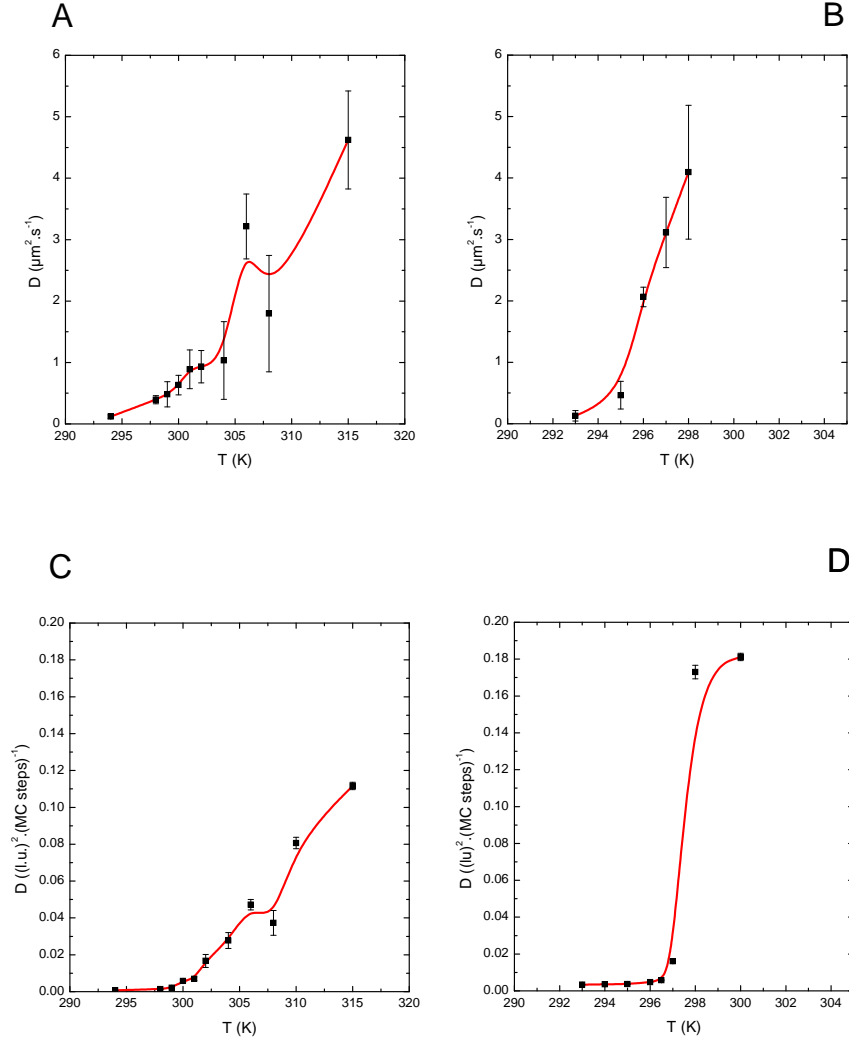


**FIGURE 10. Effective diffusion coefficient obtained by FCS diffusion laws.** Variation of the diffusion coefficient ( $D_{eff}$ ) obtained by measuring the slope of the different fits using eq. 10 of the FCS diffusion laws as a function of temperature. This clearly show, as expected, an increase in  $D$  with temperature from a lower plateau (gel phase) to a higher one (liquid phase). Part A and B are values experimentally obtained whereas part C and D are numerically obtained for DMPC:DSPC 8:2 mol:mol and pure DMPC respectively.